Design Principles of Integrated Vacuum Slot Arrangement

Jyotsna Tanwar and Madhu Vinjamur
Dept. of Chemical Engineering, Indian Institute of Technology, Bombay, Powai, Mumbai 400 076, India

L. E. Scriven
Dept. of Chemical Engineering and Materials Science, University of Minnesota, Minneapolis, MN 55455

DOI 10.1002/aic.11112
Published online February 2, 2007 in Wiley InterScience (www.interscience.wiley.com).

Coating on a substrate with a slot-die forms alternate wet and dry stripes as the substrate speed is increased when the upstream pressure equals the downstream pressure. The coating thickness is thus nonuniform across the width of the substrate. Applying vacuum upstream of the feed slot allows uniform coating at higher speeds. Different methods to apply vacuum were invented over five decades. The latest method, an integrated vacuum slot arrangement, is novel and compact. Vacuum is applied through a second slot, called vacuum slot, in the die placed upstream of the feed slot. The design principles of the arrangement are elucidated by modeling air flow in the arrangement, which is similar to liquid flow in the feed slot, but in the opposite direction. Well-accepted equations that have been derived by rigorous order of magnitude analysis to describe liquid flow have been used to model air flow. Sensitivity of the performance of the arrangement with respect to geometry is described. © 2007 American Institute of Chemical Engineers *AIChE J,* 53: 572–578, 2007
Keywords: slot-die, precision coating, vacuum slot, vacuum box

Introduction

Slot-die coating is a premetered method to coat thin and uniform liquid layers of thicknesses ranging from about 10 to few hundreds of microns. It is widely used in the production of photographic films and polymeric sheets. The cross section of slot-die coating method is shown in Figure 1. In this method, a liquid is pumped into a chamber, which distributes the liquid into a wide and narrow slot (slot height is about 100–250 microns). At the downstream end of the slot, the liquid exits into a gap (100–300 microns), called the *coating gap*, between the slot and a rotating cylinder, which moves a web or a substrate. The exiting liquid coats the web (speeds up to 2 m/s) and forms upstream and downstream menisci as shown in Figure 1. The region of the liquid bounded by the die, the substrate, and the menisci is called the *coating bead.*

As the substrate speed is increased with no pressure difference, that is, zero vacuum, the upstream meniscus of the bead moves progressively closer to the feed slot until it is reached. Any further rise in speed breaks the steady coating bead forming alternating dry and wet stripes on the substrate. The bead can also break by lowering the liquid flow. Breakup of the bead is undesirable. To delay the breakup to a higher substrate speed, reduced pressure—or "vacuum"—is usually applied to the upstream meniscus.[1] Ruschak[2] discussed the physics of the coating process at low capillary numbers when vacuum is applied. At higher capillary numbers or web speeds, the bead is always located upstream of the slot if sufficiently high vacuum is applied and the bead breaks from the downstream side.[3] This is called low flow limit.

To apply vacuum, Beguin[1] invented a vacuum box, which is a very large and cumbersome arrangement. Beguin cited several coating examples to show superior performance of a slot-die with vacuum box. Beguin claimed that a small pressure difference (up to about 1.3 kPa) between the two menisci is sufficient to raise the coating speed without breaking the bead. Air enters through the clearance in the substrate and the box and makes the vacuum across the coating bead nonuniform. There is anecdotal evidence that, as a result of

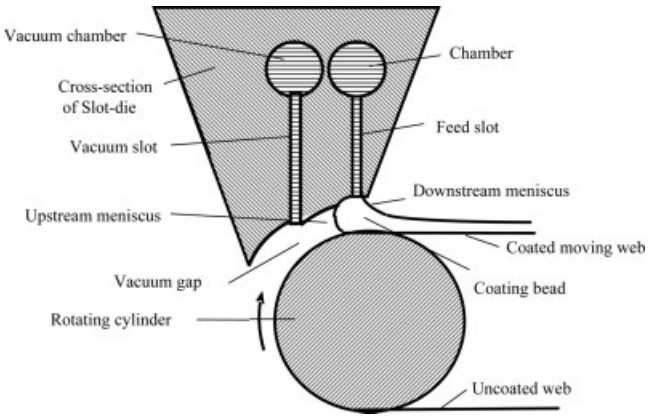

Figure 1. Cross section of slot-die with an integrated vacuum slot.

The regions between slots and cylinder and the vacuum gap are exaggerated for clarity.

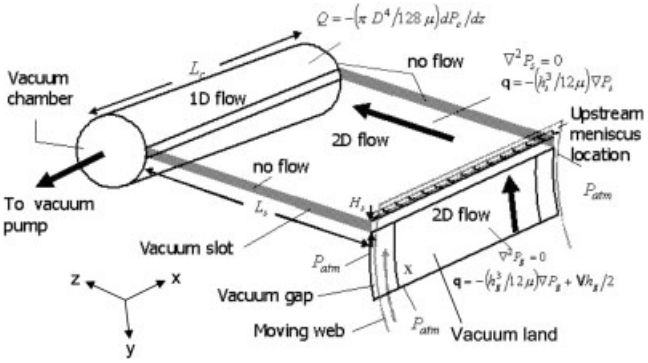

Figure 2. Integrated vacuum slot arrangement.

The solid line inside the gap indicates that only a fraction of slot-die is used for coating; the region on either side between the line and the edge acts as an overhang. The region between the upstream meniscus and the slot is ignored for modeling.

the internal air flows in some vacuum boxes, a peculiar noise is generated that can be deleterious.

Bird[4] suggested an inexpensive improvement over Beguin's vacuum box, claiming that coating speed can be increased by >50% over speeds possible by use of Beguin's method. Krussig[5] improved the vacuum arrangement invented by Bird to reduce the vortex formation in the vacuum box, which disturbs the uniformity of coating bead. Bassa[6] patented a method in which two slots are provided, one at each end of vacuum box. These slots are placed along the circumference of the cylinder that moves the substrate with uniform clearance between the slots and the substrate.

Brown and Maier[7] suggested a novel way of applying vacuum that is less cumbersome and compact than applications illustrated in earlier patents. In this method, vacuum is applied through a second slot in the die, called the *vacuum slot*, located upstream of the feed slot (Figure 1). This second slot is an integral part of the die. The vacuum slot is extended upstream to form "vacuum land." The gap between the vacuum land and the substrate is called the *vacuum gap*. Joined to the vacuum slot upstream in the die is a vacuum chamber. In an end-evacuated system, vacuum is applied at one end of the chamber; it is applied at the center of the chamber in a center-evacuated system.

Brown and Maier in their patent stated that the vacuum land could be mounted separately from the upstream region of the upstream lip. The arrangement improved die performance (increased coating speeds, coating gaps, and thinner wet coatings). They reported that the vacuum gap can be varied from 76 to 500 microns with the preferred gap being 150 microns. The vacuum land can be changed from 6.35 to 25.4 mm with the preferred length being 12.7 mm.

Figure 2 shows a three-dimensional schematic of the vacuum slot arrangement. Vacuum on the coating bead is governed by the airflow into the vacuum gap from its upstream edge and sides. When vacuum is applied, air leaks from the sides of the vacuum gap into it. From the gap, it enters the slot, and from there to the vacuum chamber and then to a vacuum source. The air leaking from the sides of the vacuum gap tends to reduce the vacuum near the ends of the coating bead. Because of the lower vacuum at the ends, the upstream meniscus reaches the feed slot at the ends first and the coating bead is likely to break there first. Then the breakdown propagates progressively toward the center.

The objective of our work is to elucidate the design principles for Brown and Maier's integrated vacuum slot arrangement. The airflow in the arrangement is similar to liquid flow in the feed slot but in the opposite direction; therefore air flow can be modeled along the same lines as those for liquid flow. Liquid flow has been analyzed extensively.[8–11] Through order-of-magnitude analysis, Weinstein and Ruschak[12] justified some of the earlier theoretical analyses. We use the well-accepted equations that describe the liquid flow to model airflow in the vacuum slot arrangement.

Sometimes only a fraction of the slot-die's width is used for coating substrate. This can be achieved by blocking a fraction of the liquid feed slot's width at either end. Then the vacuum gap on either side of the moving substrate acts as an overhang. These alter the pressure distribution and air flow in the arrangement.

In what follows, equations that describe air flow in the vacuum slot arrangement are presented. The effects of various design parameters such as slot height, gap size, vacuum land, chamber size, and the overhangs on the performance of vacuum slot arrangement are discussed.

Governing Equations

Figure 2 shows a schematic of an integrated vacuum slot arrangement. When vacuum is applied at one end of the vacuum chamber (Figure 2), air enters the slot through the vacuum gap. From the slot it flows into the vacuum chamber and to the vacuum source. The solid line in the vacuum gap shows overhangs on each side. When the die is operated at its full width the overhang length is zero. Equations for air flow in the vacuum gap, the vacuum slot, and the vacuum chamber are presented below separately. The equations are coupled at the junction between the gap and the slot and between the slot and the chamber.

Vacuum gap

Lubrication approximation accurately describes air flow in the vacuum gap because the gap is narrow (70–500

microns[7]) compared to die width and length of the vacuum land (12.7–25.4 mm[7]). Flow rate per unit width of the slot-die ($\mathbf{q_g}$) is given by

$$\mathbf{q_g} = -\left(\frac{h_g^3}{12\mu}\right)\nabla_{\mathbf{p_g}} + \frac{\mathbf{V}h_g}{2} \tag{1}$$

where h_g is vacuum gap size, μ is the viscosity of air, $\nabla\mathbf{p_g}$ is the two-dimensional pressure gradient across and along the vacuum gap (x and y directions, respectively), and $\mathbf{V}$ is the speed of the moving substrate. The first term on the right side of the Eq. 1 represents flow arising from the pressure gradient (Poiseuille flow) and the second term represents flow arising from substrate motion (Couette flow).

Lubrication approximation is valid and inertial forces are negligible if Re $\varepsilon \ll 1$, where Re $= \rho q_g/\mu$ is the Reynolds number, ρ is density, μ is viscosity, and $\varepsilon = h_g/L$ is the aspect ratio of the gap, with L being a characteristic dimension of the gap region. Equation 1 is used to estimate the Reynolds number, assuming that Couette flow is negligible compared to Poiseuille flow (which is generally the case), Re $\varepsilon = (\rho h_g^4/12\mu^2)(\Delta P/L^2)$, which is <1 for typical values of the variables involved. For $\rho = 1$ kg/m^3 and $\mu = 1.8 \times 10^{-5}$ kg/(m $\cdot$ s), $\Delta P = 10$ kPa, $h_g = 100$ microns, and L, the length of vacuum gap region $= 0.1$ m, Re $\varepsilon = 0.026$. Note that for large h_g and small L, Re ε may be comparable to one and Eq. 1 may not be applicable. Here, the resistance of the slot is neglected to estimate the flow. Including resistance of the slot would reduce both the flow and the Reynolds number.

The length of the entrance region before the flow becomes fully developed is proportional to the product of Reynolds number and gap size. Because of small gap sizes and low Reynolds numbers, the length is of the order of few millimeters, which is small compared to width and length of the vacuum gap.

In the gap, the equation of continuity holds:

$$\nabla \cdot \mathbf{q_g} = 0 \tag{2a}$$

The flow can be considered incompressible because the applied vacuum is usually low (<10 kPa). Therefore, Eq. 2a becomes

$$\nabla^2\mathbf{p_g} = 0 \qquad \text{or} \qquad \frac{\partial^2 p_g}{\partial x^2} + \frac{\partial^2 p_g}{\partial y^2} = 0 \tag{2b}$$

Through detailed order-of-magnitude analysis of the complete set of three-dimensional equations for flow in liquid feed slot, Weinstein and Ruschak[12] showed that if the slot height is small compared to its length and width, pressure distribution in the slot is described by a Laplace equation. Equation 2b is in keeping with their findings.

Pressure is atmospheric on the two sides and upstream edge of the vacuum gap. In the case of overhangs, on their top edges pressure is also atmospheric. These constitute three boundary conditions for Eq. 2; the fourth condition is at the junction between the vacuum gap and the vacuum slot where flow equations are coupled.

Pressure must be continuous at the junction between the gap and the slot ($y = 0$; $z = L_s$) and flow rates are related by continuity:

$$p_g = p_s \tag{3a}$$

$$\frac{-h_g^3}{12\mu}\frac{\partial p_g}{\partial y} + \frac{Vh_g}{2} = \frac{-h_s^3}{12\mu}\frac{\partial p_s}{\partial z} \tag{3b}$$

where p_s is pressure in the vacuum slot and h_s is height of the vacuum slot. The location of the coating bead downstream of the vacuum slot depends on liquid flow, speed of the substrate, and applied vacuum. The pinning points resulting from sharp edges are as important as the start-up procedure used to generate the coating bead in many cases. Accurate modeling should include all these variables. In this article, the region between the coating bead and the vacuum slot is neglected. This is a fairly good approximation because this region is small compared to the vacuum land.

Vacuum slot

Flow in the slot is two-dimensional in the x- and z-directions (Figure 2) because the length and width of the slot are much larger than the slot height. Lubrication approximation models air flow fairly well in the slot:

$$\mathbf{q_s} = -\left(\frac{{h_s}^3}{12\mu}\right)\nabla\mathbf{p_s} \tag{4}$$

where $\mathbf{q_s}$ is the flow rate per unit width in the slot and $\nabla\mathbf{p_s}$ is the two-dimensional pressure gradient across and along the vacuum slot (x- and z-directions, respectively). Unlike in the gap, there is no contribution to flow in the slot arising from substrate motion.

Again, as in the vacuum gap, Re $\varepsilon = (\rho h_s^4/12\mu^2)(\Delta P/L^2) \ll 1$ for Eq. 4 to hold in the slot. Slot size (h_s) is comparable to gap size but the characteristic dimension of the slot is larger than that of the gap. Therefore, Re $\varepsilon \ll 1$ and Eq. 4 accurately describes air flow in the slot. Again, the length of the entrance region is negligibly small compared to the width and length of the vacuum slot because of small slot sizes and low Reynolds numbers.

Because the flow is incompressible,

$$\nabla^2\mathbf{p_s} = 0 \qquad \text{or} \qquad \frac{\partial^2 p_s}{\partial x^2} + \frac{\partial^2 p_s}{\partial z^2} = 0 \tag{5}$$

There is no flow through the solid walls on two sides of the slot. Therefore the pressure gradient perpendicular to the walls is zero. These are two boundary conditions on Eq. 5.

At the boundary between the slot and the chamber, flow equations are coupled. Along the boundary ($0 \le x \le L_c$; $y = 0$; $z = 0$), pressure is taken to be continuous:

$$p_s = p_c \tag{6}$$

The air that leaks into the chamber locally from the slot results in local change in flow in the chamber:

$$q(x) = -\frac{dQ(x)}{dx} \qquad \text{at} \qquad y = 0;\ z = 0 \tag{7}$$

where p_c is the pressure in the chamber and Q is the flow rate in the chamber.

Vacuum chamber

The vacuum chamber is idealized as a cylinder in which flow is assumed to be one-dimensional in the axial direction. Leonard,[9] Sartor,[10] and Durst et al.[11] discussed viscous-dominated and inertial effects on the flow in the die chamber, and their work is based on one-dimensional flow there, which is widely accepted. Weinstein and Ruschak[12] showed that liquid flow in the chamber can be modeled using a one-dimensional equation, even though the flow is strictly two-dimensional because liquid diverts into the slot. Typically, the viscous forces are dominant inside the chamber for flow of liquid through it. Even for air flow, inertial forces can be neglected at low flows. Poiseuille's relation between volumetric rate (Q) and pressure gradient (dp_c/dx) approximates the flow in the vacuum chamber:

$$Q = -\frac{\pi D^4}{128\mu}\frac{dp_c}{dx} \tag{8}$$

where D is diameter of the chamber.

Inertial force is proportional to the product of density and square of the mean velocity and viscous force is proportional to pressure drop in the chamber. For laminar flow in the chamber, the mean velocity is $V = R^2\Delta P_c/8\mu L$, where R is the radius of the chamber, which is typically about a few centimeters. The ratio of the forces is

$$\frac{Inertial\ force}{Viscous\ force} = \frac{\rho R^4 \Delta P_c}{64\mu^2 L_c^2}$$

which is proportional to $\Delta P_c/{L_c}^2$. The pressure gradient across the chamber, found by solving the model equations, is negligible for typical values of R and L_c (up to a few meters). Thus, the ratio is <1 and the inertial forces can be neglected.

By combining Eqs. 7 and 8, a second-order differential equation in p_c is obtained. The two boundary conditions on the differential equations are: pressure is prescribed at one end of the chamber where vacuum is applied; at the other end, the pressure gradient is zero because the chamber is closed there:

$$P_c = P_{vac} \qquad \text{at} \qquad x = y = z = 0 \tag{9}$$

$$dP_c/dx = 0 \qquad \text{at} \qquad x = L_c;\ y = 0; z = 0 \tag{10}$$

where P_c is the pressure in the vacuum chamber, P_{vac} is the applied vacuum, and L_c is the length of the vacuum chamber.

Solution Strategy

The flow equations along with the boundary conditions are made nondimensional by using the following scaling:

$$\alpha = \frac{x}{L_c} \qquad \beta = \frac{y}{L_g} \qquad \gamma = \frac{z}{L_s}$$

$$P_1 = \frac{p_g}{P_{atm}} \qquad P_2 = \frac{p_s}{P_{atm}} \qquad P_3 = \frac{p_c}{P_{atm}}$$

where L_g is length of the vacuum land and L_s is length of the vacuum slot. Equation 2b changes to

$$\frac{\partial^2 P_1}{\partial \alpha^2} + \left(\frac{L_c}{L_g}\right)^2 \frac{\partial^2 P_1}{\partial \beta^2} = 0 \tag{11}$$

The boundary conditions are: on the two sides of vacuum land, $\alpha = 0$, $\gamma = 1$; $0 \le \beta \le 1$ and $\alpha = \gamma = 1$; and on the upstream edge of the vacuum land, $\beta = \gamma = 1$; $0 \le \alpha \le 1$, $P_1 = 1$. When overhangs are used, pressure on the two top edges of the overhangs are atmospheric:

$$P_1 = 1 \qquad \text{at} \qquad \gamma = 1;\ \beta = 0;\ 0 \le \alpha \le f\alpha$$

and

$$\gamma = 1;\ \beta = 0;\ 1 - f\alpha \le \alpha \le 1$$

where $f\alpha$ is the length of overhang on each side, which is a fraction of the total web width:

$$P_1 = P_2 \qquad \text{all along the slot}$$

Equation 3b becomes

$$\frac{\partial P_1}{\partial \beta} = \left(\frac{h_s^3}{h_g^3}\frac{L_g}{L_s}\right)\frac{\partial P_2}{\partial \gamma} + \frac{6V\mu}{h_g^2} \tag{12}$$

all across the slot where air enters $\beta = 0$; $\gamma = 1$; and $0 \le \alpha \le 1$.

The bracketed term of Eq. 12 is the ratio of resistance of the vacuum gap to flow to that of the vacuum slot. Scaling transforms Eq. 5 to

$$\frac{\partial^2 P_2}{\partial \alpha^2} + \left(\frac{L_c}{L_s}\right)^2 \frac{\partial^2 P_2}{\partial \gamma^2} = 0 \tag{13}$$

The boundary conditions on Eq. 13 are: on two sides of vacuum slot; $\alpha = 0$; $\beta = 0$; $0 \le \gamma \le 1$ and $\alpha = 1$; $\beta = 0$; $0 \le \gamma \le 1$:

$$\frac{\partial P_2}{\partial \alpha} = 0 \tag{14}$$

$$P_2 = P_3 \qquad \text{all along the chamber} \tag{15}$$

The second-order differential equation resulting from Eq. 7 becomes

$$\frac{\partial^2 P_3}{\partial \alpha^2} = -\left(\frac{32 h_s^3 L_c^2}{3\pi D^4 L_s}\right)\frac{\partial P_2}{\partial \gamma} \tag{16}$$

along the length of the chamber $\beta = \gamma = 0$; $0 \le \alpha \le 1$.

The bracketed term in the Eq. 16 is the ratio of resistance of vacuum chamber to flow to that of the slot.

At the left end of the chamber, 10 kPa vacuum is applied for a base case

$$P_3 = \frac{P_{vac}}{P_{atm}} = 0.901 \qquad \text{at} \qquad \alpha = \beta = \gamma = 0$$

and at the opposite end

$$\frac{dP_3}{d\alpha} = 0 \qquad \text{at} \qquad \alpha = 1,\ \beta = \gamma = 0 \tag{17}$$

Equations 11–17 form a set of coupled linear first- and second-order partial differential equations. This set was solved to obtain pressure in the three regions: the vacuum gap, the slot, and the chamber. Nondimensionalized equations were discretized with a finite-difference scheme, which converts them to a set of linear algebraic equations.

Second derivatives in the x- and y-directions were approximated by a five-point stencil as

$$\nabla^2 P \cong \frac{P_{i-1}^j - 2P_i^j + P_{i+1}^j}{(\Delta x)^2} + \frac{P_i^{j-1} - 2P_i^j + P_i^{j+1}}{(\Delta y)^2} + O(\Delta x^2) + O(\Delta y^2)$$

To make discretization error of order two, the first derivative was approximated by three-point stencil:

$$\frac{dP}{dx} \cong \frac{P_{i-2}^j - 4P_{i-1}^j + 3P_i^j}{2\Delta x} + O(\Delta x^2)$$

$$\frac{dP}{dx} \cong \frac{-3P_i^j + 4P_{i+1}^j - P_{i+2}^j}{2\Delta x} + O(\Delta x^2)$$

The first equation approximates boundary condition along the right edge of the vacuum slot and the second equation along the left edge. The linear algebraic equations that were obtained by finite difference approximation were arranged in the form $\underline{\underline{A}}\underline{P} = \underline{b}$, where $\underline{P}$ is the vector of pressures in all three regions.

Numbers of intervals in the x-, y-, and z-directions were chosen to be 10, 20, and 20, respectively, because doubling the number of intervals in all directions changed the relative error in pressures defined below by only 0.16%.

$$\text{Relative error} = \sqrt{\sum \left(\frac{x_i - x_j}{x_i}\right)^2}$$

where x_i represents pressures at all nodes for a given number of divisions and x_j represents pressures at the same nodes when the number of divisions was doubled in all three directions. The total number of equations solved was 681. The time taken for a typical run was 2–3 min on a machine with 512 MB memory and 4.66 GHz speed.

Results and Discussion

Two dimensionless parameters which affect the performance of integrated vacuum slot as defined earlier are: $h_s^3 L_g / h_g^3 L_s$, shown in Eq. 12, is the ratio of resistance of the vacuum gap to air flow to that of the vacuum slot and $(32 h_s^3 L_c^2 / 3\pi D^4 L_s)$, shown in Eq. 16, is the ratio of resistance of the vacuum chamber to air flow to that of the slot. For the base case, the two parameters were set to 10 and 0.1, respectively. The other dimensionless parameters, L_c/L_g and L_c/L_s were set to be 10 and 1.5, respectively. The values indicate that compared to slot resistance to flow, gap resistance is high but chamber resistance is low.

For the base case values of parameters, Figure 3 shows pressure (dimensionless) contours in an integrated vacuum slot arrangement without overhangs. On the y-axis, 0 to 1 represents vacuum gap and 1 to 2 indicates vacuum slot. The vacuum chamber is represented by $y = 2$ and vacuum is applied at the left end of the chamber. The air flows down the pressure gradient and leaks into the vacuum gap from its upstream edge and also from the sides. Except near the sides, the flow is one-dimensional along the vacuum gap. Because resistance of the vacuum gap is higher than that of the slot, the pressure drops significantly in the vacuum gap (1 to 0.93) compared to that in the slot (0.93 to 0.901) and higher vacuum is achieved on the coating bead. Also, the vacuum is nearly uniform across the bead. The arrows drawn perpendicular to the pressure contours represent air velocity vectors.

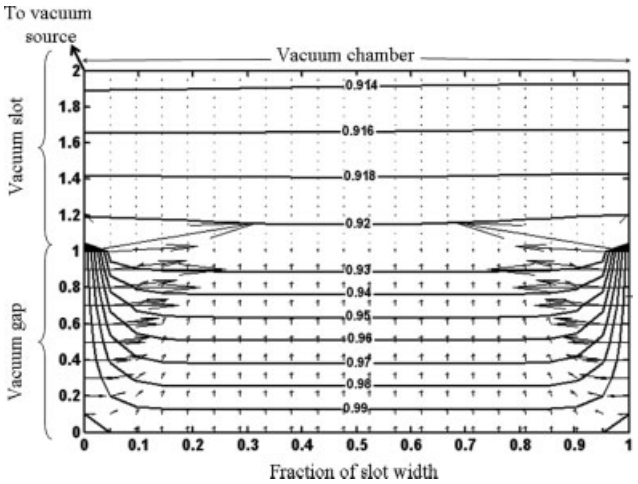

Figure 3. Pressure contours and air flow vectors in integrated vacuum slot arrangement without overhangs.

Applied vacuum is 10 kPa. Gap to slot resistance is 10 and chamber to slot resistance is 0.1. On the y-axis, 0 to 1 indicates vacuum gap and 1 to 2 represents vacuum slot.

The pressure drop in the slot is less compared to that in the gap (0.93 to 0.901). The contours indicate no flow perpendicular to the sides of the vacuum slot and that flow is unidirectional along the slot. This is because the chamber offers less resistance compared to that of the slot and thus the pressure drop across the chamber is insignificant and pressure profiles flatten toward it. If the resistance of the chamber were to be increased, the pressure would fall across the chamber and the pressure would vary both across and along the slot and the flow becomes two-dimensional in the slot. Under these conditions, the vacuum on the bead can be asymmetric, in that it is higher closer to the end where vacuum is applied.

Figure 4 shows the pressure contours in an integrated vacuum slot, for the base case parameters when a fraction of the die is used for coating and a fraction of the gap left on each side acts as overhang. The width of each overhang is taken as 15% of the total web width. With overhangs, air leaks from their top edge in addition to sides and upstream edge. The leaking air makes the flow two-dimensional in the vacuum gap and the vacuum distribution is nonuniform across the bead. Vacuum is highest at the center and lowest at the ends. The pressure drop in the gap is less compared to the case without overhangs and, thus, lower vacuum is achieved.

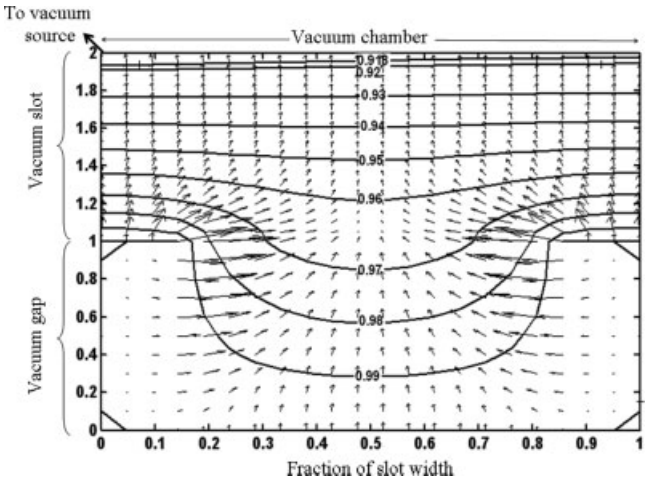

Figure 4. Pressure contours and air flow vectors in integrated vacuum slot arrangement with overhangs inside the vacuum gap.

Applied vacuum is 10 kPa. Gap to slot resistance is 10 and chamber to slot resistance is 0.1. On the *y*-axis, 0 to 1 indicates vacuum gap and 1 to 2 represents vacuum slot.

Pressure contours in the slot are similar to the case without overhangs but the pressure drop is greater in the slot with overhangs.

Vacuum ratio, one of the two indicators used in this work to assess the performance of the integrated vacuum slot, is defined as the ratio of vacuum at the center of the coating bead to the applied vacuum. As noted in Figures 3 and 4, vacuum varies across the slot (or the bead); the second performance indicator shows vacuum variation across the bead.

Figure 5 shows the sensitivity of vacuum ratio to design parameters for the arrangements with and without overhangs. The vacuum ratio increases as the resistance of the chamber is lowered and the resistance of the gap is raised, both with respect to resistance of the slot. This implies that for a given

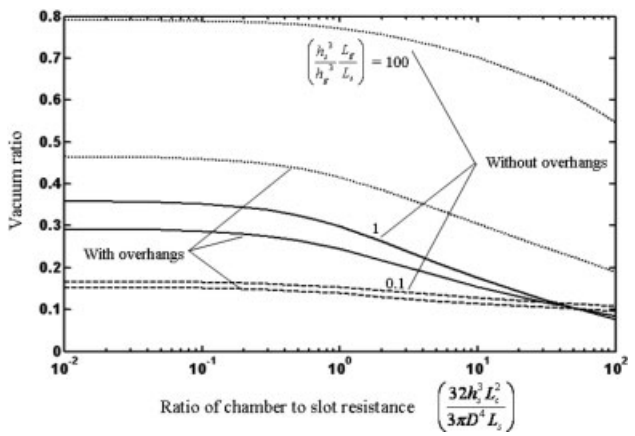

Figure 5. Effect of gap, slot, and chamber resistances on vacuum ratio for arrangements with and without overhangs.

Dots, solid line, and dashes indicate that the ratio of gap to slot resistance, $(h_s^3/h_g^3)(L_g/L_s)$, equals 100, 1, and 0.1, respectively.

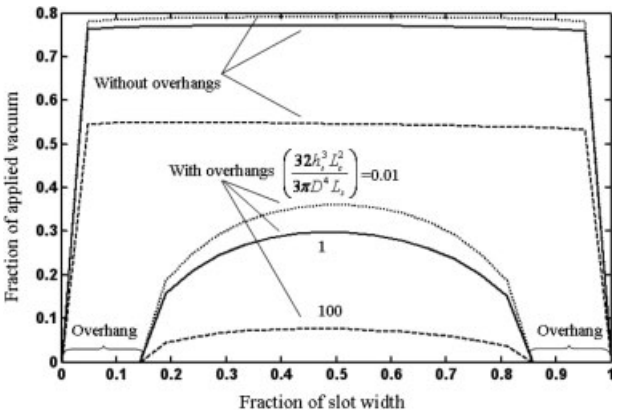

Figure 6. Effect of slot and chamber resistances on vacuum variation for arrangements with and without overhangs.

The ratio of gap to slot resistance is set to 10. Dots, solid line, and dashes indicate that the ratio of chamber to slot resistance, $32h_s^3L_c^2/3\pi D^4L_s$, equals 0.01, 1, and 100, respectively.

slot height, a larger chamber and a narrower gap increase the vacuum level on the coating bead, which is advantageous and desirable. A higher vacuum is achieved without overhangs because more air leaks into the arrangement.

As the resistance of gap is decreased, the vacuum ratio with and without overhangs is almost identical. This is because at low gap resistance the air leakage into the slot is high for both cases and the vacuum is lower. Also, for the same gap resistance, the vacuum ratio is high for lower chamber resistance. The pressure drops significantly across the chamber if the chamber resistance is raised and the vacuum ratio falls.

Figure 6 shows vacuum variation, the second performance indicator, across the bead for different values of ratio of chamber to slot resistances and for high gap to slot resistance

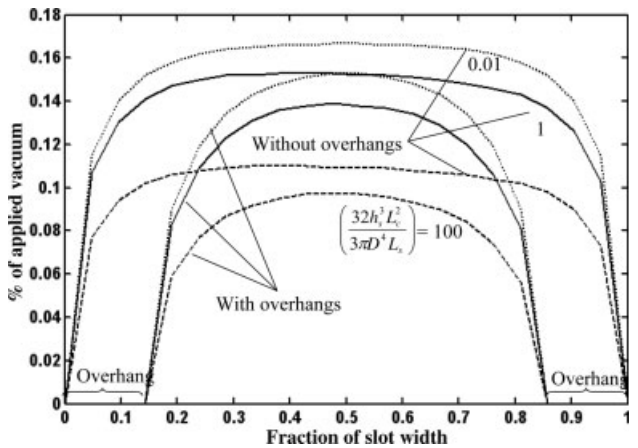

Figure 7. Effect of slot and chamber resistances on vacuum variation for arrangements with and without overhangs.

The ratio of gap to slot resistance is set to 0.1. Dots, solid line, and dashes indicate that the ratio of chamber to slot resistance, $32h_s^3L_c^2/3\pi D^4L_s$, equals 0.01, 1, and 100, respectively.

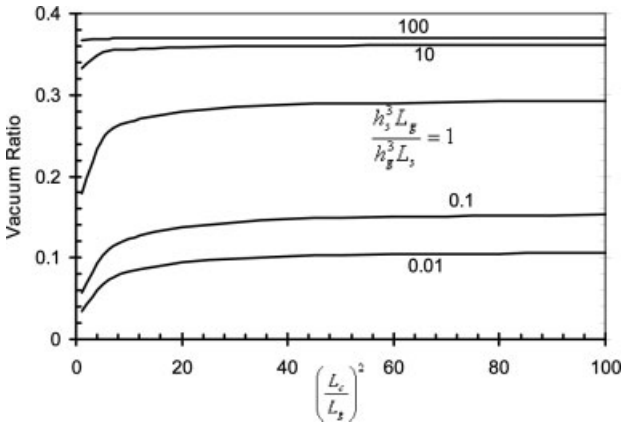

Figure 8. Effect of length of vacuum land, shown as square of ratio of length of vacuum land to width of vacuum slot, on vacuum ratio.

for the cases with and without overhangs. Vacuum is high and nearly uniform across the bead without overhangs. With overhangs, the vacuum varies more across the bead, which is highest at the center and lowest at the ends, and the vacuum is lower. When the chamber resistance is high, a lower vacuum is achieved because the pressure drops dramatically in the chamber.

Figure 7 shows vacuum variation when the gap resistance is low compared to that of the slot. More air leaks into the gap from the sides than in the arrangement where gap resistance is high. The leaking air renders the vacuum nonuniform across the bead. For a given slot, a narrower gap and a bigger chamber both achieve a nearly uniform vacuum; it is nonuniform with a wider gap and smaller chamber.

Figure 8 shows the effect of changing the length of vacuum land on the vacuum ratio. Note that the x-axis represents the square of ratio of length of vacuum land to width of the vacuum slot. As the ratio increases, or as the vacuum land becomes shorter, the vacuum ratio rises because the resistance of vacuum gap falls and more air leaks into the arrangement. When the gap to slot resistance is too high or too low, the effect on the vacuum ratio is less; at intermediate values, the effect is greater.

Overall, to achieve high and uniform vacuum, the gap resistance should be high and the chamber resistance should be low, both with respect to resistance of the slot. The values of the resistances may need to be optimized to attain a specified vacuum ratio and uniformity. The cost of accurately machining the vacuum land may be excessive because of small clearances that need to be maintained between it and the substrate. Thus, the length of the land should be small; it cannot be too small because the pressure on the bead would then be atmospheric.

Conclusions

The integrated vacuum slot arrangement in which vacuum is applied through a second lot in the die, located upstream of the feed slot, is new and more compact than earlier systems. The slot is extended downstream to form a vacuum land with a small clearance, called the vacuum gap, between the land and moving web; upstream in the die the slot is joined to a vacuum chamber. Design principles of the arrangement consisting of the slot, the gap, and the chamber have been enunciated in this work. Vacuum on the coating bead is governed by airflow in the arrangement. Dimensionless parameters that determine the ratio of resistance of the gap to the slot and the resistance of the chamber to the slot are defined. The effects of these parameters on performance of the arrangement, which indicates vacuum level on the coating bead and its uniformity across the bead, have been determined.

When gap resistance is high compared to that of the slot, high vacuum that is nearly uniform across the bead is achieved. As the gap resistance is diminished, the vacuum decreases and also becomes nonuniform. The vacuum also lessens when the chamber resistance is raised. When only a fraction of the slot-die is used for coating, the regions of vacuum gap on either side of substrate act as overhangs. With overhangs, vacuum on the bead decreases and becomes nonuniform across it. As the length of vacuum land is raised, resistance of vacuum gap rises and the vacuum ratio falls. Based on our study we conclude that with a narrow gap, wide slot, big chamber, and short vacuum land, uniform and high vacuum is obtained on the bead.

Literature Cited

1. Beguin AE. *Method of Coating Strip Material*. U.S. Patent No. 2 681 294; 1954.
2. Ruschak KJ. Limiting flow in a pre-metered coating device. *Chem Eng Sci*. 1976;31:1057–1060.
3. Carvalho MS, Kheshgi HS. Low-flow limit in slot coating: Theory and experiments. *AIChE J*. 2000;46:1907–1917.
4. Bird MG. *Apparatus for Coating a Continuous Web*. U.S. Patent No. 3 735 729; 1973.
5. Krussig KF. *Apparatus for Coating a Web with Viscous Coating Material*. U.S. Patent No. 4 335 672; 1982.
6. Bassa A. *Vacuum Box with Variable Stage Volume to Improve Coating Uniformity*. U.S. Patent No. 4 545 321; 1985.
7. Brown OD, Maier GW. *Die Coating Method and Apparatus*. U.S. Patent No. 5 639 305; 1997.
8. Vrahapoulou EP. A model for flow in dies. *Chem Eng Sci*. 1991;46:629–636.
9. Leonard WK. Inertia and gravitational effects of extrusion dies for non-Newtonian fluids. *Polym Eng Sci*. 1985;25:570–576.
10. Sartor L. *Slot Coating: Fluid Mechanics and Die Design*. PhD Thesis. Minneapolis, MN: University of Minnesota; 1990.
11. Durst FU, Lange U, Raszillier H. Optimization of distribution chambers of coating facilities. *Chem Eng Sci*. 1994;49:161–170.
12. Weinstein SJ, Ruschak KJ. One-dimensional equations governing single-cavity die design. *AIChE J*. 1996;42:2401–2414.

Manuscript received Mar. 31, 2006, and revision received Nov. 10, 2006.